

Gamma Rays from Ultracompact Primordial Dark Matter Minihalos

Pat Scott^{1,2} and Sofia Sivertsson^{1,3}

¹*Oskar Klein Centre for Cosmoparticle Physics, AlbaNova, SE-10691 Stockholm, Sweden*

²*Department of Physics, Stockholm University, AlbaNova, SE-10691 Stockholm, Sweden*

³*Department of Theoretical Physics, Royal Institute of Technology (KTH), AlbaNova, SE-10691 Stockholm, Sweden*

(Received 2 September 2009; published 20 November 2009)

Ultracompact minihalos have been proposed as a new class of dark matter structure. They would be produced by phase transitions in the early Universe or features in the inflaton potential, and constitute nonbaryonic massive compact halo objects today. We examine the prospects of detecting these minihalos in gamma rays if dark matter can self-annihilate. We compute present-day fluxes from minihalos produced in the e^+e^- annihilation epoch and the QCD and electroweak phase transitions. Even at a distance of 4 kpc, minihalos from the e^+e^- epoch would be eminently detectable today by the Fermi satellite or air Čerenkov telescopes, or even in archival *EGRET* data. Within 2 kpc, they would appear as extended sources to Fermi. At 4 kpc, minihalos from the QCD transition have similar predicted fluxes to dwarf spheroidal galaxies, so might also be detectable by present or upcoming experiments.

DOI: 10.1103/PhysRevLett.103.211301

PACS numbers: 95.35.+d, 98.70.Rz, 98.80.Cq

The identity of dark matter remains one of the key outstanding problems in physics. Weakly interacting massive particles (WIMPs) provide a compelling solution [1] because their weak-scale masses and cross sections make for a natural explanation of the observed abundance of dark matter. As most proposed WIMPs are their own antiparticles, high WIMP densities would also lead to high rates of self-annihilation. Annihilation products might then provide indirect evidence of the nature of dark matter. Gamma rays are particularly attractive in this respect, as they do not suffer the same problems of deflection and attenuation as massive, charged species.

It was proposed [2] that dark matter could be massive compact halo objects (MACHOs) of condensed baryons, e.g., brown dwarfs or faint stars. These are ruled out as the dominant component of dark matter by the cosmic microwave background (CMB; [3]), Big Bang nucleosynthesis [4], and microlensing searches [5]. Primordial black holes (PBHs) are an alternative, disfavored by their energetic evaporation, gravitational influence [6], and the large primordial density perturbations required for their production ($\delta \gtrsim 30\%$). For comparison, the initial density perturbations from inflation were $\delta \sim 10^{-5}$.

Ricotti and Gould [7] proposed a nonbaryonic MACHO that avoids these constraints and presents a promising new target for microlensing searches. Formation proceeds similarly to PBHs, whereby small-scale density perturbations in the early Universe collapse to a compact body. A small-scale power spectrum that is the same as observed on large scales [3] provides insufficient power for this to occur. Perturbations could however be enhanced by features in the inflaton potential, or phase transitions in the early Universe [8]. If a perturbation is small, matter will not be sufficiently compressed to form a black hole, leaving only a compact cloud of gas and dark matter. This mechanism requires density contrasts of just $\delta \gtrsim 10^{-3}$ to proceed so is

far more viable than PBH formation. If such ultracompact minihalos (UCMHs) exist, they will be ultradense and excellent targets for indirect detection of WIMPs [9].

Here, we investigate gamma-ray signals expected from UCMHs containing WIMP dark matter. We consider UCMHs produced in three phase transitions in the early Universe: electroweak symmetry breaking ($T_{EW} \approx 200$ GeV), QCD confinement ($T_{QCD} \approx 200$ MeV), and e^+e^- annihilation ($T_{ee} \approx 0.51$ MeV). We first discuss the masses, density profiles, and primordial abundance of UCMHs, then WIMP models and annihilation channels. We present predicted fluxes and discuss prospects for detection with satellite missions and Air Čerenkov telescopes (ACTs). In an appendix, we also give explicit predictions from a supersymmetric framework with a neutralino WIMP [10].

Following matter-radiation equality, ultracompact minihalos accrete matter by radial infall [7] as

$$M_h(z) = \delta m \left(\frac{1 + z_{eq}}{1 + z} \right), \quad (1)$$

where $M_h(z)$ is the total mass of the UCMH at redshift z , and z_{eq} is the redshift of matter-radiation equality. We assume that UCMHs at $z = 0$ grew only until $z = 10$, because by this time structure formation would have progressed sufficiently far to prevent further accretion [11]. The initial mass of the overdensity is $\delta m \equiv \delta \times M_H(z_X)$, where $M_H(z_X)$ is the horizon mass at the time of phase transition X , and in this case, $\delta = 10^{-3}$. We take $z_{eq} + 1 = 2.32 \times 10^4 \Omega_m h^2$ [12], giving $z_{eq} = 3160$ with $\Omega_m h^2 = 0.136$ from the current best fit to the CMB, large-scale structure and Type Ia supernovae [3].

During radiation domination, the horizon mass is [13]

$$M_H(z) \approx M_H(z_{eq}) \left(\frac{1 + z_{eq}}{1 + z} \right)^2. \quad (2)$$

As $T(z) \propto g_{*S}(z)^{-1/3} R(z)^{-1} \propto g_{*S}(z)^{-1/3} (1+z)$ [12], with R the scale factor of the Universe and g_{*S} the number of effective entropic degrees of freedom, this becomes

$$M_H(T) \approx M_H(T_{\text{eq}}) \left(\frac{g_{*S}(T_{\text{eq}})^{1/3} T_{\text{eq}}}{g_{*S}(T)^{1/3} T} \right)^2. \quad (3)$$

The horizon mass, temperature, and effective entropic degrees of freedom at equality can be estimated as $M_H(T_{\text{eq}}) = 6.5 \times 10^{15} (\Omega_m h^2)^{-2} = 3.5 \times 10^{17} M_\odot$ [6], $T_{\text{eq}} = 5.5 \Omega_m h^2 = 0.75$ eV and $g_{*S}(z_{\text{eq}}) = 3.91$ [12]. At the phase transitions, $g_{*S}(T_{\text{EW}}) = 107$, $g_{*S}(T_{\text{QCD}}) \approx 55$ and $g_{*S}(T_{\text{ee}}) = 10.8$ [12], giving $\delta m_{\{\text{EW}, \text{QCD}, \text{ee}\}} = \{5.4 \times 10^{-10}, 8.4 \times 10^{-4}, 3.9 \times 10^2\} M_\odot$.

The dark matter density profile in an ultracompact minihalo is [7]

$$\rho_\chi(r, z) = \frac{3f_\chi M_h(z)}{16\pi R_h(z)^{3/4} r^{9/4}}, \quad (4)$$

in the radial infall approximation. Here, the dark matter fraction is $f_\chi = \Omega_{\text{CDM}}/\Omega_m = 0.834$ [3], and

$$\left(\frac{R_h(z)}{\text{pc}} \right) = 0.019 \left(\frac{1000}{z+1} \right) \left(\frac{M_h(z)}{M_\odot} \right)^{1/3} \quad (5)$$

is the maximum extent of the UCMH at redshift z .

The dark matter in an ultracompact minihalo could be further concentrated if baryons collapse and contract the gravitational potential. We calculated the density profile after adiabatic contraction using the method of Blumenthal *et al.* [14]. This assumes that $rM(r)$ is conserved at all r , where $M(r)$ is the mass within radius r , and that orbits of the dissipationless WIMPs do not cross. We assumed that a fraction F of the total halo mass condenses to a constant-density baryonic core of radius r_{core} . We considered $F = 10^{-2}, 10^{-3}$, and $r_{\text{core}}/R_h = 5 \times 10^{-2}, 10^{-3}$. The effect of the contraction is small for the larger core radius, so we show results only for $r_{\text{core}}/R_h = 10^{-3}$. Because the induced contraction at r is given by the increase in the baryonic mass within r , the contraction caused by a constant-density baryonic core is most pronounced around the core's edge. This is in contrast to the contraction of halos around adiabatically formed black holes, where the baryons collapse to a central point, steepening the dark matter density profile at all radii. The dark matter density in the very center of a halo does not rise significantly in the contraction unless the new baryonic distribution also has a pronounced spike at the very center.

UCMHs also erode over time as dark matter annihilates away; being ultracompact and ancient, this effect is highly significant. A simple way to estimate the maximum density ρ_{max} at time t in a halo born at t_i is [15]

$$\rho(r_{\text{cut}}) \equiv \rho_{\text{max}} = \frac{m_\chi}{\langle \sigma v \rangle (t - t_i)}, \quad (6)$$

where m_χ is the WIMP mass and $\langle \sigma v \rangle$ is the annihilation cross section (multiplied by the collisional velocity and

taken in the zero-velocity limit). We truncate the density profiles at $r = r_{\text{cut}}$, setting the density within this radius equal to ρ_{max} . For UCMHs seen today, $t = 13.7$ Gyr [3]. For noncontracted UCMHs, $t_i = t(z_{\text{eq}}) = 59$ Myr [16] because they have existed since the time of equality. For contracted profiles, $t_i = t(10) = 0.49$ Gyr [16], as they were concentrated at $z = 10$.

To estimate the cosmological abundance of UCMHs, one integrates the probability distribution of primordial density perturbations between the UCMH formation threshold ($\delta \sim 10^{-3}$) and the PBH threshold ($\delta \sim 0.3$). We approximate the distribution as Gaussian [17], giving a relic density at matter-radiation equality of

$$\Omega_{\text{UCMH}}(M_H) = \int_{10^{-3}}^{0.3} \frac{\delta}{\sqrt{2\pi}\sigma(M_H)} \exp\left(-\frac{\delta^2}{2\sigma(M_H)^2}\right) d\delta. \quad (7)$$

Here, $\sigma(M_H)^2$ is the variance of perturbations at M_H . Assuming a scale-independent perturbation spectrum of index n , and normalizing to the perturbations observed in the CMB, σ can be approximated as [17]

$$\sigma(M_H) = 9.5 \times 10^{-5} (M_H/10^{56} \text{ g})^{(1-n)/4}. \quad (8)$$

On CMB scales, $n \sim 1$ [3]. However, the CMB probes only a limited number of modes. A different power law could plausibly dominate at the small scales relevant to UCMH formation; indeed, many inflationary models give a running spectral index [6], and phase transitions could produce scale-dependent features in the power spectrum [8]. The present limit at the scale of PBH/UCMH formation is $n \leq 1.25$ [17]. As they grow by a further factor of 290 [Eq. (1)] between equality and $z = 10$, UCMHs formed in the e^+e^- annihilation epoch could account for, e.g., $\sim 1\%$ of today's dark matter if $n = 1.15$. For the QCD and electroweak phase transitions, similar abundances could be obtained for $n = 1.09-1.11$.

The gamma-ray flux from WIMP annihilation, in a solid angle $\Delta\Omega$ and integrated above energy E_{th} , is

$$\Phi(E_{\text{th}}, \Delta\Omega) = \frac{1}{8\pi m_\chi^2} \sum_f \int_{E_{\text{th}}}^{m_\chi} \frac{dN_f}{dE} dE \langle \sigma_f v \rangle \times \int_{\Delta\Omega} \int_{\text{l.o.s.}} \rho^2(\Omega, l) dl d\Omega, \quad (9)$$

where dN_f/dE is the differential photon yield from the f th annihilation channel. The final integral runs over the line of sight to the halo. For a spherically symmetric halo appearing as a point source at distance d , this is

$$\Phi(E_{\text{th}}) = \frac{1}{2d^2 m_\chi^2} \sum_f \int_{E_{\text{th}}}^{m_\chi} \frac{dN_f}{dE} dE \langle \sigma_f v \rangle \int_0^{R_h} r^2 \rho^2(r) dr. \quad (10)$$

We use $d = 4$ kpc as our canonical value because the best UCMHs for microlensing searches lie towards the Galactic bulge [7], but our results can be rescaled to any d . With a

mass fraction of 1% and $2.1 \times 10^9 M_\odot$ of dark matter within 4 kpc of Earth {assuming a Navarro–Frenk–White (NFW) halo [18]}, we expect 1×10^{14} electroweak, 9×10^7 QCD or 200 e^+e^- UCMHs within 4 kpc. At 4 kpc, all UCMHs are point sources to current experiments, though below we discuss situations where they might be seen as extended objects.

In Fig. 1, we show gamma-ray fluxes from UCMHs containing WIMPs annihilating into either $b\bar{b}$ or $\mu^+\mu^-$. We computed these with parton-shower photon yields from PYTHIA 6.4 [19] in DARKSUSY 5.05 [20]. The $b\bar{b}$ channel is common in supersymmetric models, and the $\mu^+\mu^-$ channel is prominent in models which fit the *PAMELA* and *Fermi* electron excesses [21,22]. For the $b\bar{b}$ channel, we use the canonical cross section $\langle\sigma v\rangle = 3 \times 10^{-26} \text{ cm}^3 \text{ s}^{-1}$ implied by the relic density. For $\mu^+\mu^-$, we apply a boost

factor of 100, corresponding to the Sommerfeld enhancement necessary to explain the electron data in many models. If a UCMH were situated sufficiently nearby, however, its compactness might provide the required boost factor without needing any Sommerfeld enhancement.

Despite the increased density, adiabatic contraction does not greatly increase the gamma-ray flux. This is because the flux profile is dominated by the central region, which is not strongly contracted. The Sommerfeld enhancement we used for the $\mu^+\mu^-$ channel increases r_{cut} , making the flux profile less concentrated at the center and therefore more responsive to increases in density near r_{core} . If $r_{\text{core}} \ll r_{\text{cut}}$ or $r_{\text{core}} \gg r_{\text{cut}}$, this effect is absent.

In Fig. 1, we show representative point-source sensitivities of *EGRET* [23] and *Fermi* [24] above 100 MeV. Figure 2 gives the expected fluxes as a function of threshold energy, allowing for a direct comparison with the sensitivities of current and upcoming ACTs [25,26].

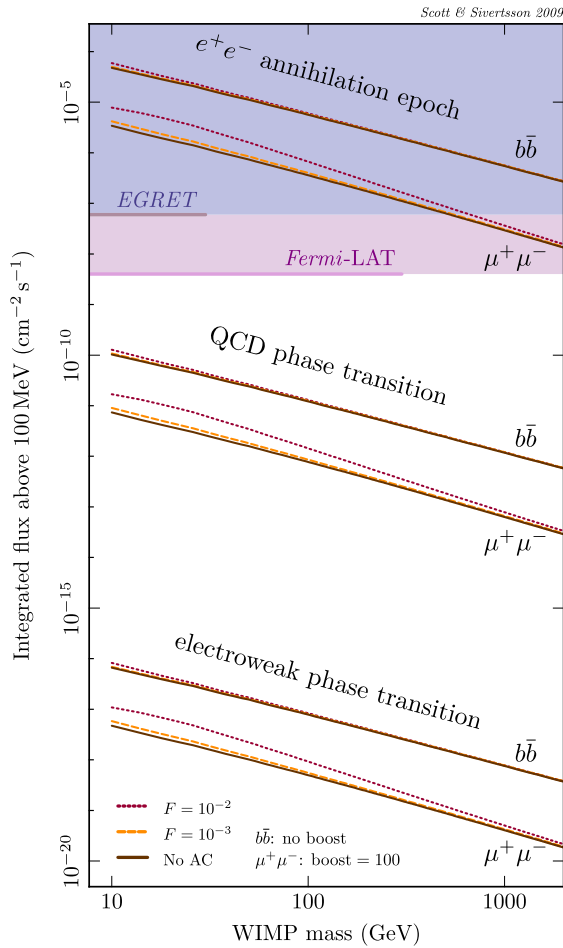


FIG. 1 (color online). Integrated fluxes above 100 MeV for UCMHs annihilating into either $b\bar{b}$ or $\mu^+\mu^-$ pairs at a distance $d = 4$ kpc. Curves are shown for different phase transitions and degrees of adiabatic contraction. Adiabatically contracted UCMHs are assumed to have a fraction F of their mass collapsed into a constant-density baryonic core of radius $10^{-3}R_h$. Also shown are approximate 5σ , power-law, high-latitude, point-source sensitivities for 2 weeks of pointed *EGRET* [23] and 1 yr of all-sky *Fermi*-LAT [24] observations. Solid limits indicate instruments’ nominal energy ranges; see also note [26].

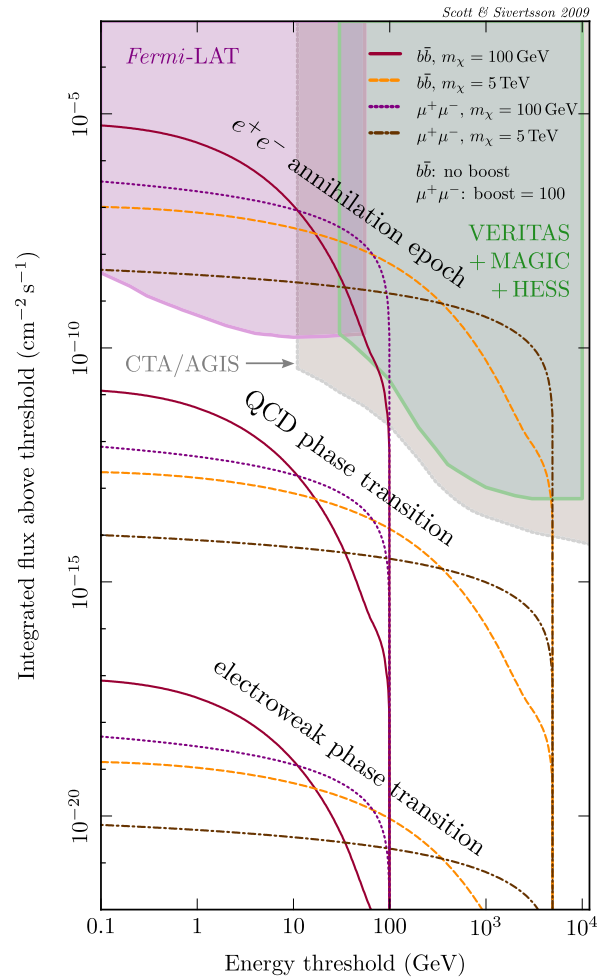


FIG. 2 (color online). Fluxes from uncontracted UCMHs at $d = 4$ kpc, as a function of the energy threshold of the observing experiment. Shaded areas show the regions accessible after a 1 yr survey by the *Fermi*-LAT [24], and 50 hr of observation by existing and planned Air Čerenkov Telescopes [25]. See also note [26].

UCMHs formed in the e^+e^- annihilation epoch should be observable by either *Fermi*, MAGIC, or HESS, depending upon the WIMP mass. They could have already been seen by *EGRET* in some cases, effectively ruling out the $b\bar{b}$ channel up to multi-TeV masses. Given their radial flux profiles, UCMHs from the e^+e^- epoch within $d \sim 2$ kpc should even appear as extended sources to *Fermi*. The nondiscovery to date of a point source with the spectral characteristics of annihilating dark matter suggests that the amplitude of perturbations generated by e^+e^- annihilation in the early Universe was $\delta < 10^{-3}$. A dedicated analysis of the *EGRET* and *Fermi* catalogues (particularly unidentified sources) is required for this statement to be made more definite. Such a study might even reveal some UCMH candidates. Limits from ACTs are more difficult to obtain, as UCMHs could have simply been missed by observing the wrong parts of the sky. On the other hand, if microlensing searches towards the Galactic bulge detect a UCMH from the e^+e^- transition, it can be definitively followed up by ACTs.

UCMHs from the QCD phase transition are not yet visible at $d = 4$ kpc, but their predicted fluxes are comparable to those of dwarf galaxies (e.g., [27]). If their abundance and the distance of the nearest example from Earth were favorable, they might be seen by *Fermi* or future instruments like the Čerenkov Telescope Array (CTA). UCMHs from the electroweak phase transition will probably not be detectable soon unless some lie within ~ 1 ly; in any case, light UCMHs might face formation problems from kinetic coupling of dark matter and free-streaming.

These results have important implications. Because of Eq. (6), the microlensing profiles of UCMHs containing WIMPs could differ from those of Ref. [7]. The additional annihilation products generated by UCMHs early in their lives could have an impact upon the ionization history of the Universe, and photons from the extra annihilation might modify the extragalactic gamma-ray background. If models explaining the *Fermi* and *PAMELA* electron excesses are accurate, UCMHs would also inject more electrons into the intergalactic medium and increase inverse Compton scattering of the CMB at all wavelengths.

We thank Joakim Edsjö, Joachim Ripken, Dave Thomson, and the anonymous referees for helpful comments, and the Swedish Research Council for funding support.

[1] L. Bergström, Rep. Prog. Phys. **63**, 793 (2000); G. Bertone, D. Hooper, and J. Silk, Phys. Rep. **405**, 279 (2005); L. Bergström New J. Phys. **11**, 105006 (2009).
 [2] B. Paczynski, Astrophys. J. **304**, 1 (1986).
 [3] E. Komatsu *et al.*, Astrophys. J. Suppl. Ser. **180**, 330 (2009).
 [4] F. Iocco, G. Mangano, G. Miele, O. Pisanti, and P.D. Serpico, Phys. Rep. **472**, 1 (2009).

[5] P. Tisserand *et al.*, Astron. Astrophys. **469**, 387 (2007); Ł. Wyrzykowski, S. Kozłowski, J. Skowron, V. Belokurov, M. C. Smith, A. Udalski, M. K. Szymański, M. Kubiak, G. Pietrzyński, and I. Soszyński *et al.*, Mon. Not. R. Astron. Soc. **397**, 1228 (2009).
 [6] A. S. Josan, A. M. Green, and K. A. Malik, Phys. Rev. D **79**, 103520 (2009).
 [7] M. Ricotti and A. Gould, arXiv:0908.0735.
 [8] C. Schmid, D. J. Schwarz, and P. Widerin, Phys. Rev. Lett. **78**, 791 (1997).
 [9] Ricotti & Gould [7] also discuss ultracompact minihalos containing PBHs, but these require similar amplitude density perturbations as PBHs, so are less appealing.
 [10] See EPAPS Document No. E-PRLTAO-103-016948 for supersymmetric (CMSSM) predictions. For more information on EPAPS, see <http://www.aip.org/pubservs/epaps.html>.
 [11] Using, e.g., $z = 30$ instead has little impact on results.
 [12] E. W. Kolb and M. S. Turner, *The Early Universe* Frontiers in Physics (Addison-Wesley, Reading, MA, 1990).
 [13] P. Coles and F. Lucchin, *Cosmology: The Origin and Evolution of Cosmic Structure* (Wiley & Sons, West Sussex, UK, 2002).
 [14] G. R. Blumenthal, S. M. Faber, R. Flores, and J. R. Primack, Astrophys. J. **301**, 27 (1986).
 [15] P. Ullio, L. Bergström, J. Edsjö, and C. Lacey, Phys. Rev. D **66**, 123502 (2002).
 [16] E. L. Wright, Publ. Astron. Soc. Pac. **118**, 1711 (2006).
 [17] A. M. Green and A. R. Liddle, Phys. Rev. D **56**, 6166 (1997).
 [18] G. Battaglia, A. Helmi, H. Morrison, P. Harding, E. W. Olszewski, M. Mateo, K. C. Freeman, J. Norris, and S. A. Shectman, Mon. Not. R. Astron. Soc. **370**, 1055 (2006).
 [19] T. Sjöstrand, S. Mrenna, and P. Skands, J. High Energy Phys. 05 (2006) 026.
 [20] P. Gondolo, J. Edsjö, P. Ullio, L. Bergström, M. Schelke, and E. A. Baltz, J. Cosmol. Astropart. Phys. 7 (2004) 8.
 [21] O. Adriani, G. C. Barbarino, G. A. Bazilevskaya, R. Bellotti, M. Boezio, E. A. Bogomolov, L. Bonechi, M. Bonghi, V. Bonvicini, and S. Bottai *et al.*, Nature (London) **458**, 607 (2009).
 [22] A. A. Abdo *et al.*, Phys. Rev. Lett. **102**, 181101 (2009).
 [23] R. C. Hartman, D. L. Bertsch, S. D. Bloom, A. W. Chen, P. Deines-Jones, J. A. Esposito, C. E. Fichtel, D. P. Friedlander, S. D. Hunter, and L. M. McDonald *et al.*, Astrophys. J. Suppl. Ser. **123**, 79 (1999).
 [24] http://fermi.gsfc.nasa.gov/ssc/data/analysis/documentation/Cicerone_/Cicerone_LAT_IRFs/LAT_sensitivity.html.
 [25] (The CTA Consortium), arXiv:0908.1410.
 [26] The sensitivities in Fig. 1 are not so accurate outside the nominal energy ranges, as heavier WIMPs in principle produce some flux outside the observable windows. The same is so for the 5 TeV lines in Fig. 2; the flux accessible to *Fermi* is probably less than shown for this mass, as part of the signal falls outside its nominal energy range. Properly extending sensitivities above the stated energy range requires a detailed spectral analysis.
 [27] G. D. Martinez, J. S. Bullock, M. Kaplinghat, L. E. Strigari, and R. Trotta, J. Cosmol. Astropart. Phys. 6 (2009) 14.